

9-15-2017

## Distinct Mechanism Evolved for Mycobacterial RNA Polymerase and Topoisomerase I Protein-Protein Interaction

Srikanth Banda

*Department of Chemistry and Biochemistry and Biomolecular Sciences Institute, Florida International University, sbanda@fiu.edu*

Nan Cao

*Department of Chemistry and Biochemistry and Biomolecular Sciences Institute, Florida International University, ncao@fiu.edu*

Yuk-Ching Tse-Dinh

*Department of Chemistry and Biochemistry and Biomolecular Sciences Institute, Florida International University, ytsedinh@fiu.edu*

Follow this and additional works at: [https://digitalcommons.fiu.edu/biomolecular\\_fac](https://digitalcommons.fiu.edu/biomolecular_fac)

---

### Recommended Citation

Banda S, Cao N, Tse-Dinh YC. Distinct Mechanism Evolved for Mycobacterial RNA Polymerase and Topoisomerase I Protein-Protein Interaction. *J Mol Biol.* 2017 Sep 15;429(19):2931-2942. doi: 10.1016/j.jmb.2017.08.011. Epub 2017 Aug 24. PMID: 28843989; PMCID: PMC5610943.

This work is brought to you for free and open access by the College of Arts, Sciences & Education at FIU Digital Commons. It has been accepted for inclusion in Biomolecular Sciences Institute: Faculty Publications by an authorized administrator of FIU Digital Commons. For more information, please contact [dcc@fiu.edu](mailto:dcc@fiu.edu).



Published in final edited form as:

*J Mol Biol.* 2017 September 15; 429(19): 2931–2942. doi:10.1016/j.jmb.2017.08.011.

## Distinct Mechanism Evolved for Mycobacterial RNA Polymerase and Topoisomerase I Protein-Protein Interaction

Srikanth Banda<sup>a,b</sup>, Nan Cao<sup>a,b</sup>, and Yuk-Ching Tse-Dinh<sup>a,b,\*</sup>

<sup>a</sup>Department of Chemistry and Biochemistry, Florida International University, Miami, Florida, USA

<sup>b</sup>Biomolecular Sciences Institute, Florida International University, Miami, Florida, USA

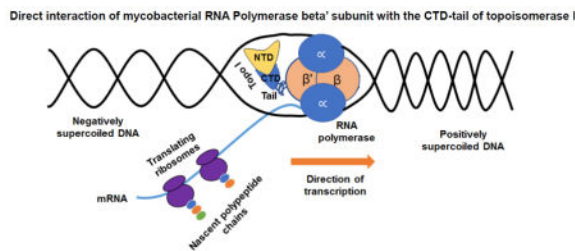
### Abstract

We report here a distinct mechanism of interaction between topoisomerase I and RNA polymerase in *Mycobacterium tuberculosis* and *Mycobacterium smegmatis* that has evolved independently from the previously characterized interaction between bacterial topoisomerase I and RNA polymerase. Bacterial DNA topoisomerase I is responsible for preventing the hyper-negative supercoiling of genomic DNA. The association of topoisomerase I with RNA polymerase during transcription elongation could efficiently relieve transcription-driven negative supercoiling. Our results demonstrate a direct physical interaction between the C-terminal domains of topoisomerase I (TopoI-CTD) and the  $\beta'$  subunit of RNA polymerase of *M. smegmatis* in the absence of DNA. The TopoI-CTD in mycobacteria are evolutionarily unrelated in amino acid sequence and three-dimensional structure to the TopoI-CTD found in the majority of bacterial species outside Actinobacteria, including *Escherichia coli*. The functional interaction between topoisomerase I and RNA polymerase has evolved independently in mycobacteria and *E. coli*, with distinctively different structural elements of TopoI-CTD utilized for this protein-protein interaction. Zinc ribbon motifs in *E. coli* TopoI-CTD are involved in the interaction with RNA polymerase. For *M. smegmatis* TopoI-CTD, a 27 amino acid tail that is rich in basic residues at the C-terminal end is responsible for the interaction with RNA polymerase. Overexpression of recombinant TopoI-CTD in *M. smegmatis* competed with the endogenous topoisomerase I for protein-protein interactions with RNA polymerase. The TopoI-CTD overexpression resulted in decreased survival following treatment with antibiotics and hydrogen peroxide, supporting the importance of the protein-protein interaction between topoisomerase I and RNA polymerase during stress response of mycobacteria.

### Graphical Abstract

\*Corresponding Authors: Yuk-Ching Tse-Dinh, ytsedinh@fiu.edu, Phone: +1 (305) 348-4956, Fax: +1 (305) 348-3772.

**Publisher's Disclaimer:** This is a PDF file of an unedited manuscript that has been accepted for publication. As a service to our customers we are providing this early version of the manuscript. The manuscript will undergo copyediting, typesetting, and review of the resulting proof before it is published in its final citable form. Please note that during the production process errors may be discovered which could affect the content, and all legal disclaimers that apply to the journal pertain.



## Keywords

TB; evolution; stress response; transcription elongation; antibiotic sensitivity

## Introduction

Topoisomerases are essential enzymes that are responsible for controlling DNA topology and facilitating vital cellular processes that include replication, transcription, recombination, and DNA repair<sup>1-5</sup>. The active site for DNA cleavage and rejoining by type IA topoisomerases is evolutionarily conserved at the N-terminal domains of bacterial topoisomerase I and topoisomerase III<sup>6, 7</sup>. Bacterial topoisomerase I is responsible for relieving the transcription-driven negative supercoiling, generated behind the RNA polymerase complex during transcription elongation<sup>8-10</sup>. The absence of topoisomerase I activity in *Escherichia coli* has been shown to result in increased R-loop formation via the stable association of the nascent transcript with the unwound DNA<sup>11, 12</sup>. This could potentially block transcription elongation<sup>13, 14</sup>. A direct association between RNA polymerase and topoisomerase I would facilitate gene expression at highly transcribed loci, including genes induced for survival in stress response.

It was previously reported that the *E. coli* RNA polymerase  $\beta'$  subunit interacts directly with the zinc ribbon and zinc ribbon-like C-terminal domains (CTD) of topoisomerase I<sup>15, 16</sup>. In *E. coli* and most bacterial species, the CTD of topoisomerase I have multiple zinc ribbon domains, each with a Zn(II) ion coordinated by four cysteines<sup>17-19</sup>. In contrast, the topoisomerase I proteins in Actinobacteria, including mycobacteria, evolved with TopoI-CTD that do not have zinc ribbon or zinc ribbon-like domains<sup>20, 21</sup>. Structural determination by X-ray crystallography showed that the *Mycobacterium tuberculosis* topoisomerase I CTD are formed by repeats of a novel protein fold of a four-stranded antiparallel  $\beta$ -sheet, stabilized by a crossing-over  $\alpha$ -helix<sup>22</sup>. We speculated that the CTD of mycobacterial topoisomerase I could be involved in protein-protein interactions, among its other functions. The protein-protein interactions of topoisomerase I from *M. smegmatis* were studied by co-immunoprecipitation (Co-IP) and pull-down assays coupled to tandem mass spectrometry<sup>23-26</sup>. The assays identified an interaction between DNA-dependent RNA polymerase (RNAP), and topoisomerase I in *M. smegmatis*. This TopoI-RNAP interaction also employed the CTD of topoisomerase I, even though the mycobacterial topoisomerase I CTD do not have zinc ribbons. The conservation of this interaction in *M. tuberculosis* with a distinct mode of protein-protein interactions was verified with further studies here.

## Results

### Identification of RNAP as protein-protein interaction partner of MsmTopoI

The protein-protein interaction network of the target protein (MsmTopoI) was first analyzed by Co-IP (Figure 1) coupled to mass spectrometry. Antibodies raised against MtbTopoI also recognized MsmTopoI (Figure S1). Following SDS-PAGE of the proteins immunoprecipitated by these antibodies from the soluble lysate of *M. smegmatis*, coomassie-stained proteins labeled as a-d in lane 5 of Figure 1B were selected. The control purified pre-immune antibodies did not precipitate the proteins corresponding to the bands a-d, as evident in lane 4 (Figure 1B). The ability of the antibodies raised against MtbTopoI to immunoprecipitate MsmTopoI from the cell lysate was confirmed by western blot analysis of the Co-IP eluates (Figure 1C). LC MS/MS analysis identified *M. smegmatis* RNAP  $\beta$  and  $\beta'$  subunits in protein band a (Supplementary material, S5).

Protein networking of MsmTopoI was further investigated by pull-down assays as described in Figure 2A with His-tagged MsmTopoI and MsmTopoI-CTD. Coomassie-stained proteins (e, f in lanes 7 and 8, Figure 2B) of *M. smegmatis* pulled down by either His-tagged MsmTopoI or MsmTopoI-CTD, but not control His-Mocr (lane 6, Figure 2B), were analyzed by LC MS/MS. *M. smegmatis* RNAP  $\beta$  and  $\beta'$  subunits were again identified in protein band e.

Protein-protein interaction between RNAP and topoisomerase I in *M. smegmatis* was further verified by reverse pull-down followed by immunoblotting (Figure 2C). In this assay, recombinant RNAP  $\beta'$  subunit (N-terminal 6xHis) was used as a bait to capture topoisomerase I from the *M. smegmatis* soluble cell lysate. The assay confirmed a concentration-dependent binding between the two proteins (lanes 3–5 in Figure 2C). The combined results from Co-IP and pull-down experiments confirmed the networking of topoisomerase I and RNAP with a distinct mode of protein-protein interaction that does not involve the zinc ribbon domains found in other bacterial topoisomerase I.

### RNAP-Topoisomerase I interactions are conserved in *M. tuberculosis* H37Rv

*M. smegmatis* is a useful model system for the understanding of processes in pathogenic *M. tuberculosis*<sup>27, 28</sup>. The protein-protein interaction between topoisomerase I and RNAP could be conserved among these mycobacteria. The RNAP-topoisomerase I interaction in *M. tuberculosis* H37Rv was studied by pull-down (Figure 3A) and Co-IP assays (Figure 3B). Results from both approaches (lane 2 in Figure 3A; lanes 2, 3 in Figure 3B) confirmed the conservation of the RNAP-topoisomerase I interaction in *M. tuberculosis*.

### Direct physical interaction between Topoisomerase I and RNAP $\beta'$ subunit

The results from the Co-IP and pull-down experiments indicate the presence of mycobacterial topoisomerase I and RNAP in the same complex. However, a direct physical interaction between these two partners in the absence of DNA or other mycobacterial proteins was not established. The direct protein-protein interactions were analyzed with purified recombinant proteins.

Physical interaction between the *M. smegmatis* RNAP  $\beta'$  subunit and topoisomerase I was demonstrated by both co-immunoprecipitation (Figure 4A) and pull-down experiments (Figure 4B). This protein-protein interaction is specific. No interaction with MsmTopoI could be observed for *M. smegmatis* RNAP  $\beta$  subunit (Figure 4A). *E. coli* topoisomerase I, with CTD that share no homology with MsmTopoI, also did not interact with the *M. smegmatis* RNAP  $\beta'$  subunit (Figure S2).

### Mapping of MsmTopoI sequence required for interaction with RNAP

Pull-down (Figure 5A) and Co-IP (Figure 5B) assays were first conducted to verify that only the CTD (D5–D8, plus tail at C-terminal end), but not the NTD (D1–D4) of MsmTopoI are involved in the protein-protein interaction with RNAP. Pull-down assays with purified recombinant His-tagged proteins retaining different regions of the CTD of MsmTopoI as bait were then used to further identify the sequence in MsmTopoI-CTD required for pull-down of RNAP (prey) from the soluble cell extract. The pull-down of RNAP (prey) by protein-protein interaction could be observed only when the full-length MsmTopoI, or MsmTopoI-CTD was used as the bait (Figure 5C; lanes 2, 8). Equal molar amounts of the bait protein (subdomains of topoisomerase I) were used in these assays. MsmTopoI-909t (D1–D8) of topoisomerase I is only missing the tail at the C-terminal end (last 27 amino acids), but it still lacks affinity for RNAP. This data indicated that the protein-protein interaction with RNAP is mediated via the C-terminal tail sequence (amino acids 910-936) of MsmTopoI (Figure 5D).

### Increased sensitivity to antibiotics and oxidative stress from overexpression of MsmTopoI-CTD

Overexpression of the MsmTopoI-CTD is expected to inhibit the interaction between native MsmTopoI and RNAP due to its competition for binding. Following tetracycline-induced overexpression of recombinant MsmTopoI-CTD in *M. smegmatis* mc<sup>2</sup> 155 (Figure 6A), less full-length MsmTopoI was pulled down by the His-tagged RNAP  $\beta'$  subunit (Figure 6B). The MsmTopoI-CTD overexpression did not affect the growth rate in 7H9 media in the absence of any stress challenge, however, growth rate was reduced by the MsmTopoI-CTD overexpression in the presence of sublethal concentration of moxifloxacin (Figure S3). Increased sensitivity to stress challenges from antibiotics (moxifloxacin, streptomycin, isoniazid) and hydrogen peroxide resulted from the MsmTopoI-CTD overexpression, as seen from the comparison of the diameters of the zones of inhibition between the control strain and MsmTopoI-CTD overexpressing strain (Figure 7A). No significant effect from MsmTopoI-CTD overexpression was observed for sensitivity to rifampicin (data not shown). This is likely because stress gene transcription is already inhibited by rifampicin. Following treatment with either moxifloxacin (0.5  $\mu$ M, 1  $\mu$ M) or hydrogen peroxide (10 mM, 20 mM), loss of viability was significantly greater for the MsmTopoI-CTD overexpressing strain when compared to the control strain (Figure 7B). These results showed that inhibition of the MsmTopoI-CTD protein-protein interactions can be correlated to enhanced sensitivity to antibiotics and oxidative stress.

## Discussion

Most bacterial species have at least two type IA topoisomerases encoded in their genome<sup>29, 30</sup> to carry out specific associated functions in replication, transcription, and recombination that require the passage of DNA through a break in a single strand of DNA<sup>3</sup>. TopoI is the only type IA topoisomerase encoded in the genomes of mycobacteria, and has been shown to be essential for the viability of both *M. tuberculosis*<sup>31, 32</sup> and *M. smegmatis*<sup>33</sup>. The identification of the protein-protein interaction partners of mycobacterial TopoI is likely to provide insights into the *in vivo* functions and regulation of this potential antibacterial target. It has been reported that the relaxation activity of MtbTopoI and MsmTopoI can be inhibited by interaction with a MazF homolog<sup>34</sup>, as well as D-ribokinase<sup>35</sup>. The catalytic activity of MtbTopoI can also be modulated by interaction with the nucleoid associated protein HU<sup>36</sup>. These previously identified protein-protein interactions may be relevant for the regulation of mycobacterial TopoI activity. However, experimental data on protein-protein interactions of mycobacterial TopoI that may inform on the physiological setting of its function<sup>37</sup> is currently not available. In this study, we tried to identify such potential partners present in the total soluble proteins of *M. smegmatis* using the approaches of Co-IP and pull-down assays coupled to mass spectrometry. RNAP was identified as a protein-protein interaction partner for MsmTopoI by both approaches. A recent ChIP-Seq study showed that *M. tuberculosis* TopoI and gyrase are recruited to genomic loci with high transcriptional activity, and MtbTopoI was localized behind RNAP to be in position for relaxing the negative supercoils generated during transcription<sup>38</sup>. Our studies here demonstrated that *M. tuberculosis* RNAP can recruit TopoI via protein-protein interaction to facilitate the co-localization during transcription elongation.

While protein-protein interaction with the RNAP  $\beta'$  subunit has been previously reported for the CTD of *E. coli* TopoI<sup>15</sup>, it should be noted that the CTD of mycobacterial TopoI share no sequence and structural similarity with the CTD of bacteria outside the Actinobacteria phylum<sup>39, 21</sup>. The CTD of *E. coli* TopoI are formed by zinc ribbon motifs stabilized by Zn(II) coordinated with four cysteines in each motif (D5–D7), or zinc ribbon-like motifs of similar structures (D8–D9)<sup>17, 18</sup>. Interaction sites for RNAP have been mapped to *E. coli* TopoI CTD regions of D5–D7 as well as D8–D9<sup>15</sup>. Analysis of the MsmTopoI protein sequence<sup>40</sup> and determination of the D1–D5 structure of MtbTopoI<sup>22</sup> have shown that the CTD of mycobacteria are formed by repeats of a distinctively different structural motif containing a  $\beta$ -sheet and  $\alpha$ -helix, with no Zn(II) present. The results reported here demonstrate that while the different bacterial species have evolved to have distinct sequences and structures of the CTD in TopoI, potentially through acquiring different duplicated gene segments during evolution<sup>41</sup>, the protein-protein interaction with the  $\beta'$  subunit of RNAP has simultaneously co-evolved through divergent mechanisms in different bacterial phylum.

Molecular simulations predicted that salt bridges and hydrogen bonds formed by basic residues positioned over a large molecular surface formed by the zinc ribbon motifs of *E. coli* TopoI are responsible for interactions with acidic residues in RNAP<sup>16</sup>. In contrast, a distinct mode of protein-protein interaction utilizing a short stretch of C-terminal tail is employed instead for the TopoI-RNAP interaction in bacteria that do not have Zn(II) binding TopoI-CTD. As shown in Figure S4, the amino acid sequence of this C-terminal tail is

highly conserved in mycobacterial TopoI and is rich in basic residues. The basic region represented by the C-terminal tail of MsmTopoI and MtbTopoI has been proposed to participate in the binding of DNA to promote strand passage during catalysis<sup>20, 42</sup>. Direct interaction of the C-terminal tail with RNAP would facilitate the rewinding of single-stranded DNA following its exit from the RNAP elongation complex to prevent stabilization of R-loop structures and inhibition of transcription elongation. The TopoI-RNAP interaction may be particularly important for efficient transcriptional response to stress conditions to achieve maximal survival following antibiotics or oxidative challenge<sup>14, 43</sup>. Competition for RNAP interaction by overexpressed recombinant MsmTopoI-CTD may have contributed to the increase in sensitivity to antibiotics and oxidative stress challenge observed here. Inhibition of the SOS response induction following moxifloxacin treatment would result in the decreased survival for the MsmTopoI-CTD overexpressing strain. Nevertheless, we cannot rule out that other protein-protein interactions inhibited by overexpressed MsmTopoI-CTD may also contribute to the increased sensitivity. Other potential protein-protein interaction partners identified in our Co-IP and pull down experiments are currently being investigated in further studies. Mycobacterial topoisomerase I may have functional roles associated with topoisomerase III in bacteria that have this additional type IA topoisomerase. The actinobacterium *Streptomyces coelicolor* also does not have topoisomerase III, and it has been hypothesized that *S. coelicolor* topoisomerase I is recruited to ParB complexes because the topoisomerase activity is needed to resolve segregating chromosomes<sup>44</sup>.

Based on the essentiality of topoisomerase I for the viability of *M. tuberculosis*, MtbTopoI is a validated target for discovery of novel TB drugs<sup>32, 45</sup>. The SOS response has been shown to be involved in the induction of mycobacterial resistance to fluoroquinolones<sup>46</sup>. Due to its involvement in transcriptional response to stress challenges, mycobacterial topoisomerase I inhibitors could be especially useful for use in combination with other antibiotics to increase the efficacy, and decrease the induction of drug resistance.

## Materials and methods

### Bacterial strains, plasmids, and cloning

*M. smegmatis* mc<sup>2</sup> 155 was obtained from ATCC and cultured in 7H9 broth. *M. tuberculosis* H37Rv genomic DNA and whole cell lysates were obtained from BEI Resources. A plasmid pMsmTopoI-CTD for overexpression of topoisomerase I-CTD in *M. smegmatis* was constructed by first placing *M. smegmatis* *topA* coding sequence (amplified with primers shown in Table S1) under the control of the tetracycline inducible TetRO promoter in pKW08 vector<sup>47</sup> via Gibson Assembly cloning<sup>48</sup>. Plasmid pMsmTopoI-CTD was then constructed for overexpression of the C-terminal domains D5–D8 plus tail (residues 627–936) by deleting the N-terminal domains D1–D4 (residues 1–626) via site-directed mutagenesis. Overexpression of the various domains of *M. smegmatis* topoisomerase I (MsmTopoI) in *E. coli* BL21 STAR DE3 (Invitrogen) was achieved with pET His6 Mocr TEV LIC cloning vector (20-T, Addgene Plasmid# 29710). Cloning of recombinant *M. tuberculosis* topoisomerase I (MtbTopoI) and its CTD in vector pLIC-HK<sup>49</sup> for expression in *E. coli* BL21-CodonPlus(DE3)-RP (Agilent) was described previously<sup>50</sup>. Coding

sequences for *M. smegmatis* RNAP  $\beta$  (RpoB) and  $\beta'$  (RpoC) subunits were inserted by Gibson cloning into the SspI site of pLIC-HK, and transformed into *E. coli* SoluBL21 (Genlantis) cells for protein expression and purification. The PCR primers used in the cloning and site-directed mutagenesis are listed in the Supplementary Information (Table S1 and Table S2).

### Protein expression and purification

DNA topoisomerase I, sub-domains of topoisomerase I, RNAP  $\beta$ , and RNAP  $\beta'$  subunits were purified as recombinant proteins for protein-protein interaction studies. Overexpression of these recombinant proteins in the *E. coli* hosts was induced with 1 mM IPTG. Following the overexpression and cell lysis, recombinant proteins were purified to near homogeneity by affinity chromatography using Ni-Sepharose 6 Fast flow beads (GE Healthcare Life Sciences), followed by size-exclusion chromatography.

### Co-Immunoprecipitation (Co-IP)/Tandem Mass spectrometry

The complex of *M. smegmatis* topoisomerase I (MsmTopoI) and its potential protein partners was isolated from the *M. smegmatis* soluble cell lysate by Co-IP<sup>23</sup>. *M. smegmatis* mc<sup>2</sup> 155 was grown to stationary phase in LB-Tween 80 (0.1%). The pelleted cells were resuspended in lysis/wash buffer (50 mM NaCl, 50 mM NaH<sub>2</sub>PO<sub>4</sub>, pH 8.0, 0.1% NP-40), and then subjected to 5 pulses of sonication (10 seconds/pulse at medium intensity). The lysate was spun at 16000×g for an hour, and the supernatant soluble lysate was used as prey in the Co-IP assays. The soluble lysate was pre-incubated (pre-cleared) with protein A/G plus agarose beads to remove proteins that bind non-specifically to the beads. The pre-cleared lysate (total protein=500  $\mu$ g) was first mixed with IgG (10  $\mu$ g) purified from serum of a rabbit inoculated with MtbTopoI or control pre-immune serum. These rabbit polyclonal antibodies cross react with MsmTopoI (Figure S1). The protein A/G plus agarose beads (Santa Cruz Biotechnology), previously equilibrated in wash buffer, was then added to the lysate-antibody reaction and left overnight at 4°C. On the following day, the reaction mixture was spun at 700×g, and the supernatant was discarded. The bead pellet with the bound proteins was washed three times in the wash buffer. The elution of the proteins bound to the beads was carried out by suspending the bead pellet in 4X SDS sample buffer (240 mM Tris-HCl, 8% SDS, 40% glycerol, 0.04% bromophenol blue), and heating at 95°C for 2 minutes. The eluted proteins (MsmTopoI, and its potential protein partners) were stained with coomassie blue following SDS-PAGE. The protein bands of interest were excised for characterization by tryptic digest and mass spectrometry (nano LC/MS/MS) at the Proteomics and Mass Spectrometry Facility of University of Massachusetts Medical School. The MS/MS results were searched using Mascot (Matrix Science, London, UK; version 2.5.0) against the UniProt\_MSmegmatis\_071714 database for trypsin digestion products.

### Pull-down assay/Tandem Mass spectrometry

For the pull-down assay<sup>24</sup>, the target protein (MsmTopoI) with a fusion tag (N-terminal 6xHistidine) was mixed with *M. smegmatis* mc<sup>2</sup> 155 soluble cell extract for 2 hours at 4°C, and then immobilized on a HisPur Cobalt agarose resin (ThermoFisher). The resin with bound target proteins was washed three times in a pull-down wash buffer (10 mM HEPES, pH 7.5, 10 mM imidazole, 0.005% Tween-20) to remove the weakly retained proteins. The



proteins that remained bound to the resin were eluted with pull-down elution buffer (10 mM HEPES, pH 7.5, 350 mM imidazole), separated by SDS-PAGE, and stained with coomassie blue. The protein bands of interest were excised for identification by tryptic digest and nano LC/MS/MS.

### Reverse pull-down assay/Immunoblotting

A reverse pull-down assay was used to validate the protein interactions identified by pull-down assays. In this assay, a recombinant *M. smegmatis* RNAP  $\beta'$  subunit (N-terminal 6xHistidine) was used as bait to pull down topoisomerase I from the soluble cell extract. The pull-down protocol was similar to that described in the previous section. Western blot analysis with rabbit polyclonal antibodies against MtbTopoI was used to detect the presence of topoisomerase I in the eluate.

### Pull-down, Co-IP assays on *M. tuberculosis* (H37Rv) cell extract

The conservation of RNAP-topoisomerase I protein-protein interactions in *M. tuberculosis* was verified by pull-down and Co-IP assays. Whole cell extract of *M. tuberculosis* H37Rv was provided by BEI Resources. The extract was spun at 16000 $\times$ g for 20 min at 4°C, and the soluble protein fraction was used for the assays. Recombinant MtbTopoI with N-terminal 6x-Histidine was used in the pull-down assay, while antibodies against topoisomerase I were used in the Co-IP assay as bait to determine if RNAP could be captured from the cell extract. Following SDS-PAGE, the proteins in the eluates from the assays were immunoblotted with a monoclonal antibody against RNAP  $\beta$  (Biolegend) which can recognize the RNAP  $\beta$  subunits<sup>51</sup> across multiple species, including *M. tuberculosis* and *M. smegmatis*.

### Effect of TopoI-CTD overexpression on sensitivity to antibiotics or hydrogen peroxide

The *M. smegmatis* strain overexpressing the CTD of topoisomerase I from the plasmid pMsmTopA-CTD, or a control *M. smegmatis* strain transformed with the cloning vector, were cultured to stationary phase in 7H9 medium containing Hygromycin (100 $\mu$ g/ml) and tetracycline (25ng/ml). The cultures were adjusted to OD<sub>600</sub>=1.0 in 7H9 medium, and 200 $\mu$ l of the OD-adjusted culture was spread on LB plates. Antibiotic or H<sub>2</sub>O<sub>2</sub> was applied to paper discs placed at the center of the plates, followed by incubation at 37°C for 60 hrs. The diameter of the zone of inhibition was measured.

For comparison of viable colony counts following stress challenge, the *M. smegmatis* strains were grown in Luria broth-Tween 80 (0.1%) containing Hygromycin (100 $\mu$ g/ml) and tetracycline (25ng/ml). At the exponential phase, the cultures were treated with moxifloxacin (0.5  $\mu$ M or 1  $\mu$ M) for 12 hours at 37°C. The treated cultures and untreated cultures were serially diluted and spread on LB plates. The viable colonies were counted, and the relative viability ratio (treated versus untreated) was calculated. Similarly, viable colony counts following treatment with hydrogen peroxide (10 mM or 20 mM) was analyzed with the strains cultured in 7H9 medium containing Hygromycin (100  $\mu$ g/ml) and tetracycline (25 ng/ml).

## Supplementary Material

Refer to Web version on PubMed Central for supplementary material.

## Acknowledgments

### Funding

This work was supported by the National Institute of Health grants GM054226 and AI069313 to YT.

We are grateful to BEI Resources for providing the *M. tuberculosis* H37Rv genomic DNA and whole cell lysate. We thank Shayna Sandhaus for proof-reading of manuscript. Plasmid pKW08-Lx was a gift from Brian Robertson (Addgene plasmid # 25012). We thank Shayna Sandhaus for proof-reading of manuscript.

## Abbreviations

<b>CTD</b>	C-terminal domains
<b>TopoI-CTD</b>	Topoisomerase I C-terminal domains
<b>MsmTopoI</b>	<i>Mycobacterium smegmatis</i> topoisomerase I
<b>MtbTopo1</b>	<i>Mycobacterium tuberculosis</i> topoisomerase I
<b>Co-IP</b>	Co-immunoprecipitation
<b>RNAP</b>	RNA polymerase

## References

- Chen SH, Chan NL, Hsieh TS. New mechanistic and functional insights into DNA topoisomerases. *Annu Rev Biochem.* 2013; 82:139–170. DOI: 10.1146/annurev-biochem-061809-100002 [PubMed: 23495937]
- Vos SM, Tretter EM, Schmidt BH, Berger JM. All tangled up: how cells direct, manage and exploit topoisomerase function. *Nat Rev Mol Cell Biol.* 2011; 12:827–841. DOI: 10.1038/nrm3228 [PubMed: 22108601]
- Wang JC. Cellular roles of DNA topoisomerases: a molecular perspective. *Nat Rev Mol Cell Biol.* 2002; 3:430–440. [doi]; nrm831 [pii]. DOI: 10.1038/nrm831 [PubMed: 12042765]
- Baranello L, Levens D, Gupta A, Kouzine F. The importance of being supercoiled: how DNA mechanics regulate dynamic processes. *Biochim Biophys Acta.* 2012; 1819:632–638. DOI: 10.1016/j.bbtagm.2011.12.007 [PubMed: 22233557]
- Dorman CJ, Dorman MJ. DNA supercoiling is a fundamental regulatory principle in the control of bacterial gene expression. *Biophys Rev.* 2016; 8:89–100. DOI: 10.1007/s12551-016-0238-2 [PubMed: 28510216]
- Baker NM, Rajan R, Mondragon A. Structural studies of type I topoisomerases. *Nucleic Acids Res.* 2009; 37:693–701. DOI: 10.1093/nar/gkn1009 [PubMed: 19106140]
- Capranico G, Marinello J, Chillemi G. Type I DNA Topoisomerases. *J Med Chem.* 2017; 60:2169–2192. DOI: 10.1021/acs.jmedchem.6b00966 [PubMed: 28072526]
- Liu LF, Wang JC. Supercoiling of the DNA template during transcription. *Proc Natl Acad Sci U S A.* 1987; 84:7024–7027. [PubMed: 2823250]
- Masse E, Drolet M. Relaxation of transcription-induced negative supercoiling is an essential function of *Escherichia coli* DNA topoisomerase I. *J Biol Chem.* 1999; 274:16654–16658. [PubMed: 10347233]

10. Wu HY, Shyy SH, Wang JC, Liu LF. Transcription generates positively and negatively supercoiled domains in the template. *Cell*. 1988; 53:433–440. 0092-8674(88)90163-8 [pii]. [PubMed: 2835168]
11. Drolet M, Phoenix P, Menzel R, Masse E, Liu LF, Crouch RJ. Overexpression of RNase H partially complements the growth defect of an *Escherichia coli* delta topA mutant: R-loop formation is a major problem in the absence of DNA topoisomerase I. *Proc Natl Acad Sci U S A*. 1995; 92:3526–3530. [PubMed: 7536935]
12. Masse E, Drolet M. R-loop-dependent hypernegative supercoiling in *Escherichia coli* topA mutants preferentially occurs at low temperatures and correlates with growth inhibition. *J Mol Biol*. 1999; 294:321–332. [doi]; S0022-2836(99)93264-3 [pii]. DOI: 10.1006/jmbi.1999.3264 [PubMed: 10610761]
13. Hraiky C, Raymond MA, Drolet M. RNase H overproduction corrects a defect at the level of transcription elongation during rRNA synthesis in the absence of DNA topoisomerase I in *Escherichia coli*. *J Biol Chem*. 2000; 275:11257–11263. [PubMed: 10753935]
14. Drolet M. Growth inhibition mediated by excess negative supercoiling: the interplay between transcription elongation, R-loop formation and DNA topology. *Mol Microbiol*. 2006; 59:723–730. MMI5006 [pii]; DOI: 10.1111/j.1365-2958.2005.05006.x [PubMed: 16420346]
15. Cheng B, Zhu CX, Ji C, Ahumada A, Tse-Dinh YC. Direct interaction between *Escherichia coli* RNA polymerase and the zinc ribbon domains of DNA topoisomerase I. *J Biol Chem*. 2003; 278:30705–30710. [doi]; M303403200 [pii]. DOI: 10.1074/jbc.M303403200 [PubMed: 12788950]
16. Tiwari PB, Chapagain PP, Banda S, Darici Y, Uren A, Tse-Dinh YC. Characterization of molecular interactions between *Escherichia coli* RNA polymerase and topoisomerase I by molecular simulations. *FEBS Lett*. 2016; 590:2844–2851. [doi]. DOI: 10.1002/1873-3468.12321 [PubMed: 27448274]
17. Grishin NV. C-terminal domains of *Escherichia coli* topoisomerase I belong to the zinc-ribbon superfamily. *J Mol Biol*. 2000; 299:1165–1177. DOI: 10.1006/jmbi.2000.3841 [PubMed: 10873443]
18. Tse-Dinh YC, Beran-Steed RK. *Escherichia coli* DNA topoisomerase I is a zinc metalloprotein with three repetitive zinc-binding domains. *J Biol Chem*. 1988; 263:15857–15859. [PubMed: 2846526]
19. Suerbaum S, Brauer-Steppkes T, Labigne A, Cameron B, Drlica K. Topoisomerase I of *Helicobacter pylori*: juxtaposition with a flagellin gene (flaB) and functional requirement of a fourth zinc finger motif. *Gene*. 1998; 210:151–161. [PubMed: 9524255]
20. Ahmed W, Bhat AG, Leelaram MN, Menon S, Nagaraja V. Carboxyl terminal domain basic amino acids of mycobacterial topoisomerase I bind DNA to promote strand passage. *Nucleic Acids Res*. 2013; 41:7462–7471. [doi]. DOI: 10.1093/nar/gkt506 [PubMed: 23771144]
21. Sikder D, Nagaraja V. Determination of the recognition sequence of *Mycobacterium smegmatis* topoisomerase I on mycobacterial genomic sequences. *Nucleic Acids Res*. 2000; 28:1830–1837. [PubMed: 10734203]
22. Tan K, Cao N, Cheng B, Joachimiak A, Tse-Dinh YC. Insights from the Structure of *Mycobacterium tuberculosis* Topoisomerase I with a Novel Protein Fold. *J Mol Biol*. 2016; 428:182–193. [doi]. DOI: 10.1016/j.jmb.2015.11.024 [PubMed: 26655023]
23. Free RB, Hazelwood LA, Sibley DR. Identifying novel protein-protein interactions using co-immunoprecipitation and mass spectroscopy. *Curr Protoc Neurosci*. 2009; Chapter 5(Unit 5.28) [doi]. doi: 10.1002/0471142301.ns0528s46
24. Brymora A, Valova VA, Robinson PJ. Protein-protein interactions identified by pull-down experiments and mass spectrometry. *Curr Protoc Cell Biol*. 2004; Chapter 17(Unit 17.5) [doi]. doi: 10.1002/0471143030.cb1705s22
25. Ning Z, Hawley B, Chiang CK, Seebun D, Figeys D. Detecting protein-protein interactions/complex components using mass spectrometry coupled techniques. *Methods Mol Biol*. 2014; 1164:1–13. [doi]. DOI: 10.1007/978-1-4939-0805-9\_1 [PubMed: 24927830]
26. Speth C, Toledo-Filho LA, Laubinger S. Immunoprecipitation-based analysis of protein-protein interactions. *Methods Mol Biol*. 2014; 1158:175–185. [doi]. DOI: 10.1007/978-1-4939-0700-7\_11 [PubMed: 24792051]

27. Shiloh MU, Champion PA. To catch a killer. What can mycobacterial models teach us about *Mycobacterium tuberculosis* pathogenesis? *Curr Opin Microbiol.* 2010; 13:86–92. [doi]. DOI: 10.1016/j.mib.2009.11.006 [PubMed: 20036184]
28. Agrawal P, Miryala S, Varshney U. Use of *Mycobacterium smegmatis* deficient in ADP-ribosyltransferase as surrogate for *Mycobacterium tuberculosis* in drug testing and mutation analysis. *PLoS One.* 2015; 10:e0122076. [doi]. doi: 10.1371/journal.pone.0122076 [PubMed: 25874691]
29. Forterre P, Gribaldo S, Gabelle D, Serre MC. Origin and evolution of DNA topoisomerases. *Biochimie.* 2007; 89:427–446. DOI: 10.1016/j.biochi.2006.12.009 [PubMed: 17293019]
30. Forterre P, Gabelle D. Phylogenomics of DNA topoisomerases: their origin and putative roles in the emergence of modern organisms. *Nucleic Acids Res.* 2009; 37:679–692. DOI: 10.1093/nar/gkp032 [PubMed: 19208647]
31. Ahmed W, Menon S, Godbole AA, Karthik PV, Nagaraja V. Conditional silencing of topoisomerase I gene of *Mycobacterium tuberculosis* validates its essentiality for cell survival. *FEMS Microbiol Lett.* 2014; 353:116–123. [doi]. DOI: 10.1111/1574-6968.12412 [PubMed: 24593153]
32. Ravishankar S, Ambady A, Awasthy D, Mudugal NV, Menasinakai S, Jatheendranath S, Guptha S, Sharma S, Balakrishnan G, Nandishaiah R, Ramachandran V, Eyermann CJ, Reck F, Rudrapatna S, Sambandamurthy VK, Sharma UK. Genetic and chemical validation identifies *Mycobacterium tuberculosis* topoisomerase I as an attractive anti-tubercular target. *Tuberculosis (Edinb).* 2015; 95:589–598. [doi]. DOI: 10.1016/j.tube.2015.05.004 [PubMed: 26073894]
33. Ahmed W, Menon S, Karthik PV, Nagaraja V. Reduction in DNA topoisomerase I level affects growth, phenotype and nucleoid architecture of *Mycobacterium smegmatis*. *Microbiology.* 2015; 161:341–353. [doi]. DOI: 10.1099/mic.0.000014 [PubMed: 25516959]
34. Huang F, He ZG. Characterization of an interplay between a *Mycobacterium tuberculosis* MazF homolog, Rv1495 and its sole DNA topoisomerase I. *Nucleic Acids Res.* 2010; 38:8219–8230. DOI: 10.1093/nar/gkq737 [PubMed: 20724443]
35. Yang Q, Liu Y, Huang F, He ZG. Physical and functional interaction between D-ribokinase and topoisomerase I has opposite effects on their respective activity in *Mycobacterium smegmatis* and *Mycobacterium tuberculosis*. *Arch Biochem Biophys.* 2011; 512:135–142. DOI: 10.1016/j.abb.2011.05.018 [PubMed: 21683681]
36. Ghosh S, Mallick B, Nagaraja V. Direct regulation of topoisomerase activity by a nucleoid-associated protein. *Nucleic Acids Res.* 2014; 42:11156–11165. [doi]. DOI: 10.1093/nar/gku804 [PubMed: 25200077]
37. Zhang C, Freddolino PL, Zhang Y. COFACTOR: improved protein function prediction by combining structure, sequence and protein-protein interaction information. *Nucleic Acids Res.* 2017; [doi]. doi: 10.1093/nar/gkx366
38. Ahmed W, Sala C, Hegde SR, Jha RK, Cole ST, Nagaraja V. Transcription facilitated genome-wide recruitment of topoisomerase I and DNA gyrase. *PLoS Genet.* 2017; 13:e1006754. [doi]. doi: 10.1371/journal.pgen.1006754 [PubMed: 28463980]
39. Szafran MJ, Strick T, Strzalka A, Zakrzewska-Czerwinska J, Jakimowicz D. A highly processive topoisomerase I: studies at the single-molecule level. *Nucleic Acids Res.* 2014 gku494 [pii].
40. Bhaduri T, Bagui TK, Sikder D, Nagaraja V. DNA topoisomerase I from *Mycobacterium smegmatis*. An enzyme with distinct features. *J Biol Chem.* 1998; 273:13925–13932. [PubMed: 9593741]
41. Viard T, de la Tour CB. Type IA topoisomerases: a simple puzzle? *Biochimie.* 2007; 89:456–467. DOI: 10.1016/j.biochi.2006.10.013 [PubMed: 17141394]
42. Jain P, Nagaraja V. Indispensable, functionally complementing N and C-terminal domains constitute site-specific topoisomerase I. *J Mol Biol.* 2006; 357:1409–1421. DOI: 10.1016/j.jmb.2006.01.079 [PubMed: 16490213]
43. Rui S, Tse-Dinh YC. Topoisomerase function during bacterial responses to environmental challenge. *Front Biosci.* 2003; 8:d256–63. [PubMed: 12456368]
44. Szafran M, Skut P, Ditkowski B, Ginda K, Chandra G, Zakrzewska-Czerwinska J, Jakimowicz D. Topoisomerase I (TopA) is recruited to ParB complexes and is required for proper chromosome

- organization during *Streptomyces coelicolor* sporulation. J Bacteriol. 2013; doi: 10.1128/JB.00798-13
45. Nagaraja V, Godbole AA, Henderson SR, Maxwell A. DNA topoisomerase I and DNA gyrase as targets for TB therapy. Drug Discov Today. 2017; 22:510–518. S1359-6446(16)30422-6 [pii]. [PubMed: 27856347]
  46. Malik M, Chavda K, Zhao X, Shah N, Hussain S, Kurepina N, Kreiswirth BN, Kerns RJ, Drlica K. Induction of mycobacterial resistance to quinolone class antimicrobials. Antimicrob Agents Chemother. 2012; 56:3879–3887. [doi]. DOI: 10.1128/AAC.00474-12 [PubMed: 22564842]
  47. Williams KJ, Joyce G, Robertson BD. Improved mycobacterial tetracycline inducible vectors. Plasmid. 2010; 64:69–73. DOI: 10.1016/j.plasmid.2010.04.003 [PubMed: 20434484]
  48. Gibson DG. Enzymatic assembly of overlapping DNA fragments. Methods Enzymol. 2011; 498:349–361. [doi]. DOI: 10.1016/B978-0-12-385120-8.00015-2 [PubMed: 21601685]
  49. Doyle SA. High-throughput cloning for proteomics research. Methods Mol Biol. 2005; 310:107–113. [PubMed: 16350949]
  50. Annamalai T, Dani N, Cheng B, Tse-Dinh YC. Analysis of DNA relaxation and cleavage activities of recombinant *Mycobacterium tuberculosis* DNA topoisomerase I from a new expression and purification protocol. BMC Biochem. 2009; 10:18. doi: 10.1186/1471-2091-10-18 [PubMed: 19519900]
  51. Burgess RR, Thompson NE. Advances in gentle immunoaffinity chromatography. Curr Opin Biotechnol. 2002; 13:304–308. S0958166902003403 [pii]. [PubMed: 12323350]

### Highlights

- Mycobacteria topoisomerase I interacting protein partner of functional significance
- Mycobacteria topoisomerase I interacts directly with RNA polymerase beta' subunit
- Interaction via short C-terminal tail instead of Zn ribbon motifs in other bacteria
- Antibiotics hypersensitivity from topoisomerase I C-terminal domain overexpression
- Convergent evolution of topoisomerase I-RNAP interaction via distinct mechanism

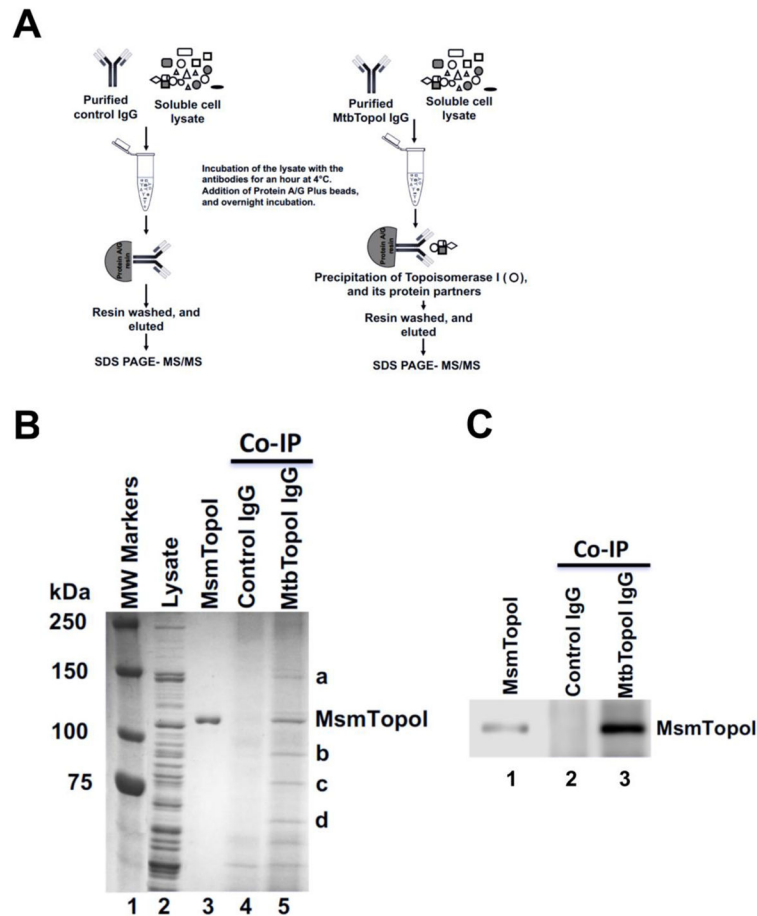


**Figure 1. Co-Immunoprecipitation of topoisomerase I and interacting proteins from *M. smegmatis* lysate**

(A) Schematic of the Co-IP. (B) Proteins were stained with coomassie blue following SDS-PAGE. Lane 1: MW standards; Lane 2: 15  $\mu$ g of total *M. smegmatis* proteins in soluble lysate; Lane 3: purified recombinant MsmTopoI. Proteins were immunoprecipitated from *M. smegmatis* lysate (500  $\mu$ g total proteins) by pre-immune rabbit antibodies (lane 4) or antibodies raised against MtbTopoI (lane 5). Bands a-d were selected for LC MS/MS analysis. (C) A fraction of the eluates from Co-IP reactions were electrophoresed on a SDS-PAGE and immunoblotted with TopoI antibodies. Lane 1: 25 ng of purified MsmTopoI. The efficiency of the Co-IP assay was verified by analyzing a small fraction of eluates from the reaction of *M. smegmatis* lysate with pre-immune rabbit antibodies (lane 2), or antibodies raised against MtbTopoI (lane 3).

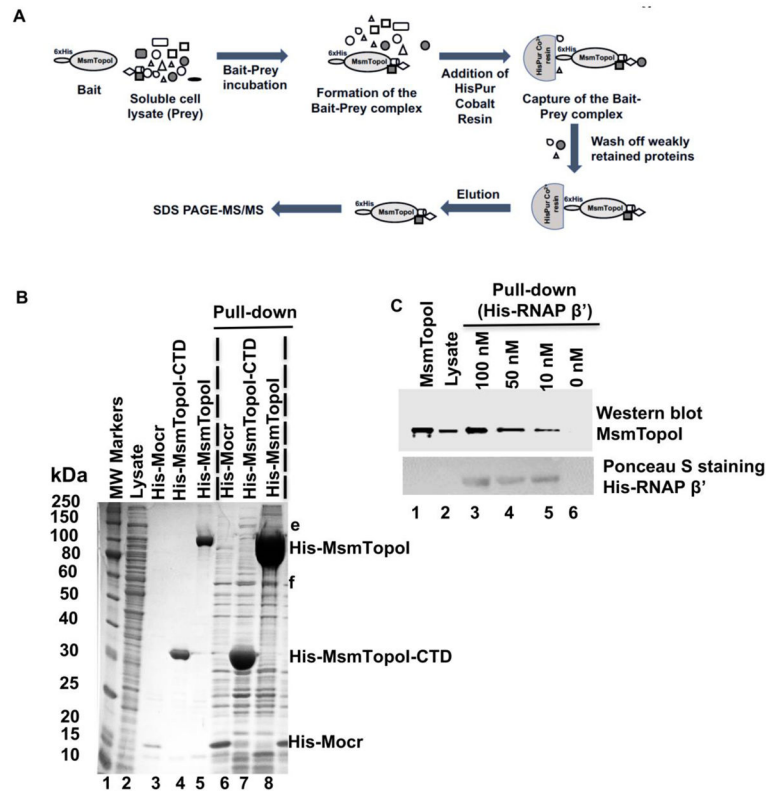


**Figure 2. Pull-down assay of MsmTopoI-RNAP interaction with HisPur Cobalt agarose resin** (A) General scheme of the pull-down assay. (B) Proteins pulled down from *M. smegmatis* soluble lysate by recombinant N-terminal His-tagged MsmTopoI (lane 8) or MsmTopoI-CTD (lane 7). His-Mocr, a recombinant viral protein, was used as bait in the control reaction (lane 6). Lane 1: MW standards; Lane 2: purified recombinant His-Mocr; Lane 3: purified recombinant His-MsmTopoI-CTD; Lane 4: purified recombinant His-MsmTopoI. (C) Reverse pull-down of TopoI from *M. smegmatis* soluble lysate with purified recombinant RNAP  $\beta'$  subunit (N-terminal His-tagged). Following SDS-PAGE, the proteins eluted from the HisPur Cobalt were analyzed by western blot using anti-TopoI antibodies. Lane 1: purified recombinant MsmTopoI (100 ng); Lane 2: 15  $\mu$ g of total proteins in *M. smegmatis* soluble lysate; Lanes 3–6: eluates from pull-down assay using 500  $\mu$ g of total proteins in *M. smegmatis* soluble lysate with His-tagged RNAP  $\beta'$  subunit of concentrations 100 nM (lane 3), 50 nM (lane 4), 10 nM (lane 5), and 0 nM (lane 6). The nitrocellulose membrane was also stained with Ponceau S for detection of the recombinant bait (His-tagged RNAP  $\beta'$ ) used in the assay.



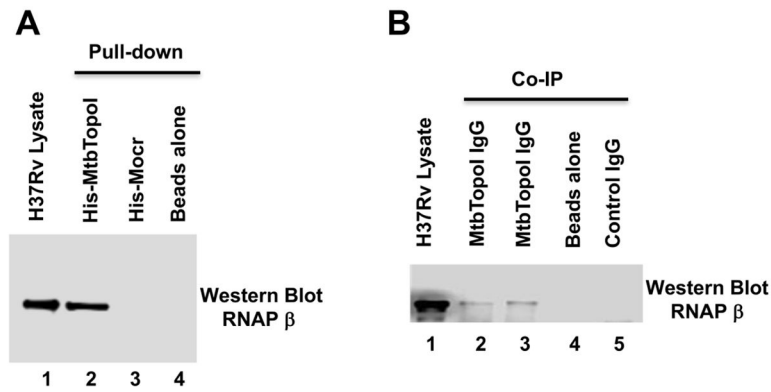


**Figure 3. *M. tuberculosis* H37Rv topoisomerase I and RNAP are protein-protein interaction partners**

*M. tuberculosis* RNAP was detected by western blot using a monoclonal antibody against *E. coli* RNAP  $\beta$  subunit that cross-reacts with mycobacterial RNAP. (A) Pull-down assay. Lane 1: total soluble lysate of *M. tuberculosis* H37Rv (10  $\mu$ g). Eluates from HisPur cobalt resin incubated with 250  $\mu$ g of lysate and purified His-tagged MtbTopoI (lane 2), 6xHisMocr (lane 3) or without any His-tagged protein (lane 4). (B) Co-Immunoprecipitation assay. Lane 1: total soluble lysate of *M. tuberculosis* H37Rv (10  $\mu$ g). Immunoprecipitates from 250  $\mu$ g of total soluble lysates incubated with IgG against MtbTopoI (lanes 2, 3), no IgG added (lane 4), and IgG from pre-immune serum (lane 5) were analyzed by western blot with the antibody recognizing RNAP  $\beta$  subunit.

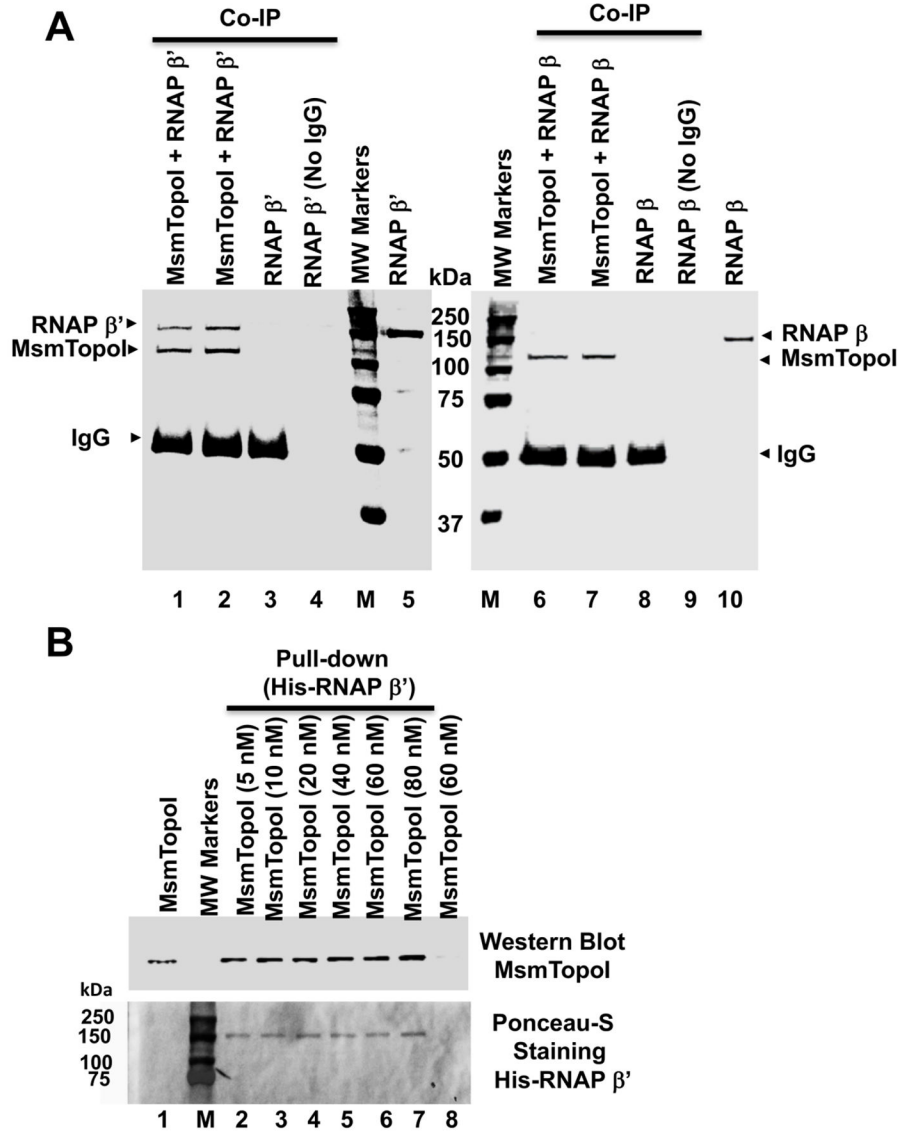


**Figure 4. Direct physical interaction between purified *M. smegmatis* topoisomerase I and RNAP  $\beta'$  subunit**

(A) Purified RNAP  $\beta'$  subunit (lanes 1–4), but not  $\beta$  subunit (lanes 6–9), can be co-immunoprecipitated with MsmTopoI. The co-immunoprecipitation reaction contained 100 nM (lanes 1, 6) or 200 nM of MsmTopo I (lanes 2, 7), along with 125 nM of  $\beta'$  (lanes 1–4) or  $\beta$  (lanes 6–9) subunit of RNAP. Lanes 3, 8: no MsmTopoI added; Lanes 4, 9: no IgG added; Lanes 5, 10: purified RNAP subunit (1.5  $\mu$ g). The proteins in the gel were stained with coomassie blue following SDS-PAGE. M: Molecular weight standards. (B) Pull-down assay with HisPur cobalt resin. Lane 1: 25 ng of MsmTopoI. The pull-down reactions contained 15 nM of His-RNAP  $\beta'$  subunit incubated with 5, 10, 20, 40, 60, 80 nM (lanes 2–7) of MsmTopoI. Lane 8: control of 60 nM MsmTopoI with no RNAP  $\beta'$  subunit added. MsmTopoI pulled down by His-RNAP  $\beta'$  subunit was visualized by western blot. The nitrocellulose membrane was then stained with Ponceau S. M: Protein molecular weight standards.

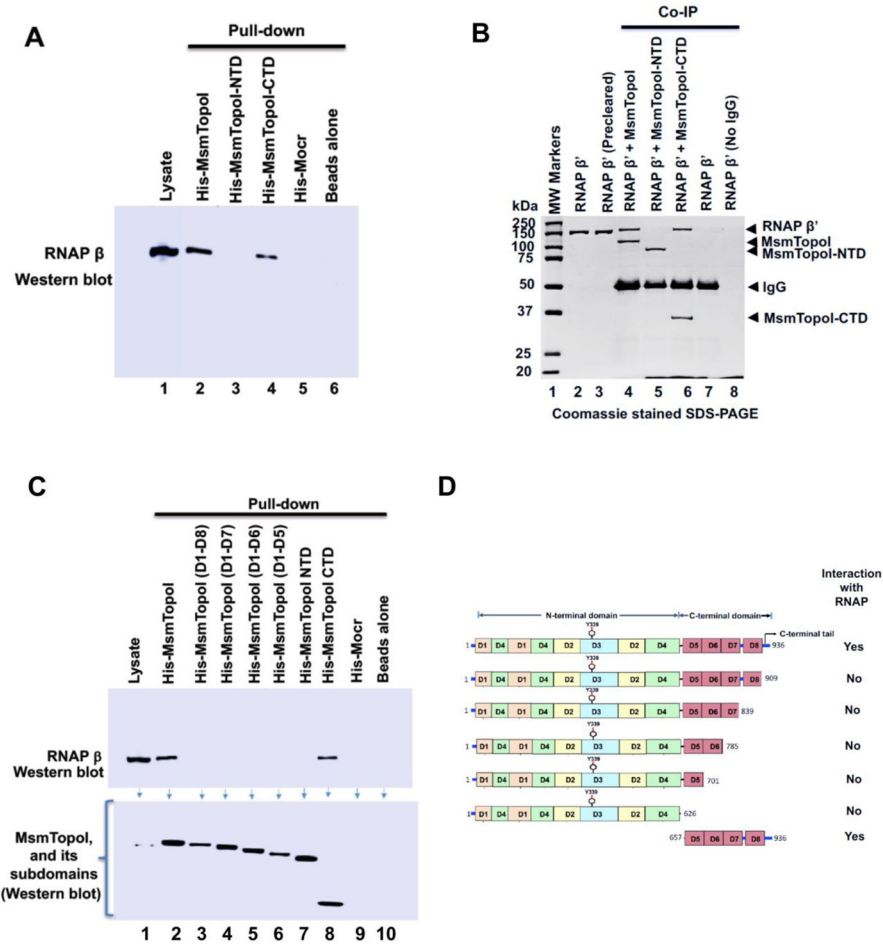


**Figure 5. Identification of MsmTopoI sequence required for interaction with RNAP**  
 (A) *M. smegmatis* soluble lysate was incubated with the His-tagged recombinant MsmTopoI or its fragment, and the eluates from the reaction were analyzed by western blotting. TopoI-CTD, but not TopoI-NTD, can interact with RNAP in *M. smegmatis* cell lysate. (B) Direct physical interaction between TopoI-CTD and RNAP  $\beta'$  subunit was verified by Co-IP assay. Purified RNAP  $\beta'$  subunit was incubated with MsmTopoI or its fragment, and the proteins immunoprecipitated by TopoI antibodies from the reactions were analyzed by SDS-PAGE/coomassie staining. The assay confirms a physical interaction of RNAP  $\beta'$  with MsmTopoI-CTD (lane 6), and not MsmTopoI-NTD (lane 5). Purified RNAP  $\beta'$ , by itself, did not bind to the antibody (lane 7) or the beads (lane 8). (C) Pull-down assay with MsmTopoI truncation mutants lacking different segments of the TopoI-CTD. *M. smegmatis* soluble lysate was incubated with different constructs of the recombinant MsmTopoI, and the eluates were probed for the presence of RNAP. The full-length recombinant MsmTopoI (lane 2), and CTD-MsmTopoI (lane 8) can interact with RNAP. (D) Domain arrangement of MsmTopoI is shown here. The results from pull-down and Co-IP assays, taken together, demonstrate that the tail at the C-terminal end of MsmTopoI interacts with RNAP.

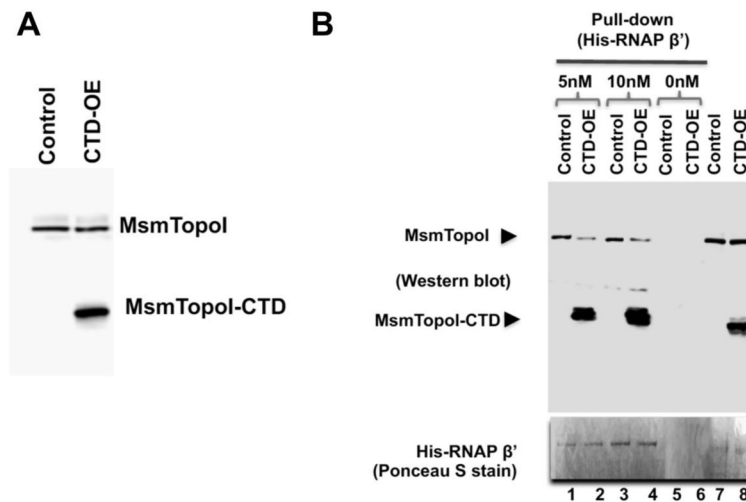


**Figure 6. Inhibition of MsmTopoI-RNAP interaction with overexpression of recombinant MsmTopoI-CTD**

(A) The tetracycline-induced overexpression of MsmTopoI-CTD was confirmed by western blot analysis with rabbit polyclonal antibodies against TopoI. Lane 1: lysate (10  $\mu$ g) of *M. smegmatis* transformed with control vector. Lane 2: lysate (10  $\mu$ g) of *M. smegmatis* transformed with pMsmTopoI-CTD. (B) Pull-down of MsmTopoI from *M. smegmatis* lysate by His-tagged RNAP  $\beta'$  subunit is reduced by the competing overexpressed MsmTopoI-CTD. Pull-down of MsmTopoI and MsmTopoI-CTD from the lysate (350  $\mu$ g) by His-RNAP  $\beta'$  (5 nM or 10 nM) was analyzed by western blot using antibodies against MtbTopoI (upper panel). Lanes 1, 3: pull-down reactions with lysate from the strain transformed with the control vector (control) in the presence of 5 nM His-RNAP  $\beta'$  or 10 nM His-RNAP  $\beta'$ . Lanes 2, 4: pull-down reactions with lysate from the strain overexpressing the MsmTopoI-CTD (CTD-OE) in the presence of 5 nM His-RNAP  $\beta'$  or 10 nM His-RNAP  $\beta'$ . Lanes 5, 6: lysates from either the control strain or the overexpression strain were incubated with the beads as a negative control for the pull-down assays. Lane 7: lysate (10  $\mu$ g) from *M. smegmatis* transformed with the control vector. Lane 8: lysate (10  $\mu$ g) from *M. smegmatis* overexpressing the MsmTopoI-CTD. The nitrocellulose membrane was stained with Ponceau S (bottom panel) for the detection of the bait (His-RNAP  $\beta'$ ).

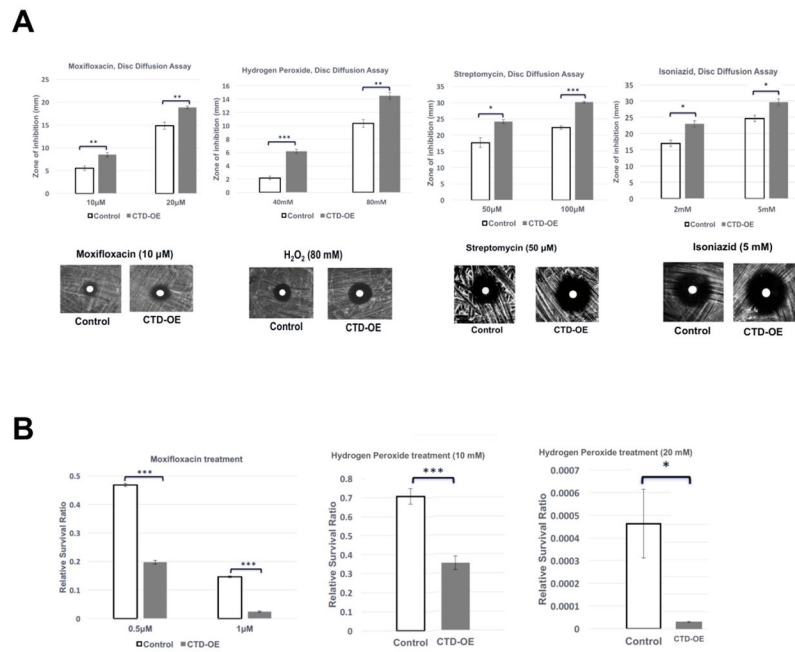


**Figure 7. Effect of TopoI-CTD overexpression on sensitivity of *M. smegmatis* to stress challenge** (A) The tetracycline-induced cultures of the vector control strain (control), and the MsmTopoI CTD-overexpression strain (CTD-OE) were spread on LB plates, and a blank paper disc was placed on the plate. 20  $\mu$ L of the antibiotic solution or hydrogen peroxide was added to the disc. The plates were incubated at 37°C for 60 hours, and the zone of inhibition was measured. Error bars represent the standard deviation (n=3). Student's t-test was used to calculate the p-values (\* p<0.05; \*\* p<0.005, \*\*\*p<0.0005). (B) Following treatment with moxifloxacin or hydrogen peroxide for 12 hours, the untreated and treated cultures of the tetracycline-induced vector control strain (control), and MsmTopoI CTD-overexpression (CTD-OE) strain were serially diluted and spread on LB plates. The viable colony counts (CFU/ml) were determined to calculate the relative survival ratios as the colony counts of the treated cultures divided by the colony counts of the untreated cultures.